Modern Pathology (2021) 34:798–807
https://doi.org/10.1038/s41379-020-00702-9

ARTICLE

Prognostic impact of tumor microvessels in intrahepatic cholangiocarcinoma: association with tumor-infiltrating lymphocytes

Kyohei Yugawa[1,2] · Shinji Itoh[1] · Tomoharu Yoshizumi[1] · Norifumi Iseda[1] · Takahiro Tomiyama[1] · Takeo Toshima[1] · Noboru Harada[1] · Kenichi Kohashi[2] · Yoshinao Oda[2] · Masaki Mori[1]

Received: 26 June 2020 / Revised: 18 September 2020 / Accepted: 5 October 2020 / Published online: 19 October 2020

Abstract

Tumor microvessel density (MVD) is a prognostic factor for patients with intrahepatic cholangiocarcinoma (ICC). Tumor-infiltrating lymphocytes (TILs) are also key components of the tumor microenvironment that play important roles in ICC progression. This study aimed to clarify the relationships between the MVD and immune status and prognosis in patients with ICC. Immunohistochemical staining for cluster of differentiation 34 (CD34), cluster of differentiation 8 (CD8), forkhead box protein P3 (Foxp3), and programmed death-ligand 1 (PD-L1) was performed. The relationships between the MVD and clinicopathological characteristics and outcomes were analyzed. Additionally, the correlations between the MVD, CD8+ and Foxp3+ TIL counts, and PD-L1 expression were evaluated. One hundred ICC patients were classified into high ($n = 50$) and low ($n = 50$) MVD groups. The serum platelet and carbohydrate antigen 19-9 levels were higher in the low MVD group than in the high MVD group ($P = 0.017$ and $P = 0.008$, respectively). The low MVD group showed a significantly larger tumor size ($P = 0.016$), more frequent microvascular invasion ($P = 0.001$), and a higher rate of intrahepatic ($P = 0.023$) and lymph node ($P < 0.001$) metastasis than the high MVD group. Moreover, the MVD showed a high positive correlation with CD8+ TILs ($r = 0.754$, $P < 0.001$) and a negative correlation with Foxp3+ TILs ($r = -0.302$, $P = 0.003$). In contrast, no significant correlation was observed between the MVD and PD-L1 expression in cancer cells ($P = 0.817$). Patients with low MVDs had a significantly worse prognosis than those with high MVDs. Furthermore, multivariable analyses revealed that a low MVD influenced recurrence-free survival. A decreased intratumoral MVD might predict ICC patient outcomes. Tumor microvessels might be associated with ICC progression, possibly by altering TIL recruitment.

Introduction

Intrahepatic cholangiocarcinoma (ICC) is the second most common primary liver tumor after hepatocellular carcinoma (HCC) and a major cause of cancer mortality and morbidity worldwide [1]. ICCs are estimated to account for ~5–15% of all primary liver cancers, and their incidence has been increasing worldwide [2]. Although surgical resection is a potentially curative treatment that improves ICC patient outcomes, many patients are at risk of recurrence. Combined systemic chemotherapy or radiotherapy has been shown to help improve the outcomes for patients who have undergone hepatic resection for ICC; however, their prognosis remains poor because of tumor progression. Recently, several reports have identified predictive tumor-specific factors, including tumor, lymph node, metastasis (TNM) classification, tumor differentiation, and vascular invasion [3, 4]. However, the predictive risk factors that influence recurrence among ICC patients have not been fully investigated.

The tumor microenvironment (TME) is known to play an important role in ICC progression [5]. The abundant

Supplementary information The online version of this article (https://doi.org/10.1038/s41379-020-00702-9) contains supplementary material, which is available to authorized users.

✉ Shinji Itoh
itoshin@surg2.med.kyushu-u.ac.jp

[1] Department of Surgery and Science, Graduate School of Medical Sciences, Kyushu University, Fukuoka 812-8582, Japan

[2] Department of Anatomic Pathology, Graduate School of Medical Sciences, Kyushu University, Fukuoka 812-8582, Japan

desmoplastic stroma contains different nonimmune and immune cells, including cancer-associated fibroblasts [6], tumor-associated macrophages [7], endothelial cells (ECs) [8], and lymphocytes [9], which are correlated with a poor prognosis or immune response. Previously, an increasing number of studies reported that tumor angiogenesis is related to ICC progression. However, the detailed mechanism underlying the role of the microvessel density (MVD) in ICC progression and its clinical usefulness as a predictive factor remain poorly understood.

Tumor-infiltrating lymphocytes (TILs) play a pivotal role in tumor progression. In addition, the evaluation of TILs can predict the outcomes of several cancer patients. Cluster of differentiation (CD) 8-positive T lymphocytes, known as cytotoxic T lymphocytes, are key immune cells that kill cancer cells by releasing perforin and granzymes [10]. The transcription factor forkhead box protein P3 (Foxp3) is a specific marker of regulatory T lymphocytes. Foxp3+ T lymphocytes exert an immune suppressive function by producing several immune inhibitory cytokines [11]. Recent studies have shown the relationships between the densities of CD8+ and Foxp3+ TILs and patient prognosis in several cancers [12–14]. In ICC, few studies have reported that CD8+ and Foxp3+ T lymphocytes are associated with a poor prognosis [15, 16]. More recently, immune checkpoint blockade has been predicted to be an effective treatment for several solid tumors. Programmed cell death-ligand 1 (PD-L1) also plays a crucial role in tumor immunobiology in ICC [17]. However, the relationship between tumor microvessels and immune cells in ICC has not been fully elucidated. This study aimed to investigate the relationship between the MVD and tumor progression, focusing on tumor microvessels and immune status in the TME.

Materials and methods

Patients and specimen preparation

All consecutive patients with ICC who had undergone hepatic resection from September 1992 to November 2019 at Kyushu University Hospital in Japan were enrolled. The patients who had undergone resection for primary ICC without preoperative chemotherapy or radiation were selected retrospectively. The samples included resected liver specimens from these patients. Preoperation and postoperation de-identified clinical information were obtained from electronic and paper records. Complete charts for clinical data were available for all patients, and consent for research use of their resected tissue was obtained. To evaluate the histological features, the specimens were fixed in 10% formalin solution, embedded in paraffin, and sectioned into 4-μm-thick slices. In addition, this study was approved by the ethics committee of our hospital according to the ethical guidelines of the Japanese government (approval number: 30–454).

Evaluation of TILs, fibrosis, and necrosis

The percentage of TILs was assessed based on H&E staining according to a previously reported standardized methodology for scoring TILs in solid tumors [18]. TILs were evaluated in the tumor cell compartment under light microscopy (×200 magnification, ×20 objective lens, and ×10 ocular lens; 0.950 mm^2 per field). All sections from each ICC patient were reviewed. The most fibrotic and necrotic areas within the tumor were selected at low magnification (×40), and then the fibrosis and necrosis grades were evaluated in a representative field at high magnification (×200). The fibrotic component was divided into the following three categories: mild, <10%; moderate, 10–60%; and severe, more than 60% of the tumor. The grade of necrosis was defined as positive when it occupied more than 10% of the tumor and negative when it was absent. Histological evaluations were performed independently by two observers (KY and KK) who were blinded to the clinical background of the subjected patients. If the difference between the data was more than 10%, it was recalculated. The average finding of the two observers was taken as the final histological data.

Immunohistochemical analysis

The sliced sections were deparaffinized in xylene and rehydrated in a graded series of ethanol. Subsequently, the specimens were subjected to antigen retrieval [37 °C incubation for 30 min, 0.2% trypsin in 0.01 mol/L phosphate-buffered saline for cluster of differentiation 34 (CD34) staining; 98 °C incubation by microwave for 20 min, Tris-EDTA buffer (pH 9.0) for CD8 and Foxp3 staining; and 120 °C incubation by autoclave for 10 min, Tris-EDTA buffer (pH 9.0) for PD-L1 staining]. Next, the specimens were treated with 0.3% H_2O_2 for 5 min to inhibit the endogenous peroxidase activity. The primary antibodies, including a mouse monoclonal anti-CD34 antibody (Clone QBEnd 10; Agilent Technologies, Santa Clara, CA, USA), mouse monoclonal anti-CD8 antibody (Clone C8/144B; Agilent Technologies), mouse monoclonal anti-Foxp3 antibody (236A/E7; Abcam, Cambridge, UK), and rabbit monoclonal anti-PD-L1 antibody (E1L3N; Cell Signaling Technology, Danvers, MA, USA), were applied to the specimens at a dilution of 1:100 and incubated overnight at 4 °C. The next day, the specimens were incubated with labeled streptavidin–biotin for 1 h at room temperature. Color development was performed using 3,3′-diaminobenzidine, followed by counterstaining with Mayer's hematoxylin.

All sliced sections from each patient were reviewed by two observers (KY and KK) and representative areas of the invasive component of the tumor were selected from sections stained with H&E. One section from each paraffin block per tumor was selected for immunohistochemical staining. The average MVD detected by CD34 staining was determined for the five areas of the tumor with the highest vascular density in the intratumoral area by counting the CD34-positive microvessels under light microscopy (×200 magnification, ×20 objective lens, and ×10 ocular lens; 0.950 mm^2 per field). The average CD8+ and Foxp3+ TIL counts were calculated for the five areas with the highest staining density in the intratumoral area by counting CD8+ and Foxp3+ T cells under light microscopy (×400 magnification, ×40 objective lens, and ×10 ocular lens; 0.237 mm^2 per field). Immunohistochemical evaluations were performed independently by two observers (KY and KK) who were blinded to the clinical background of the subjected patients. If the difference between the data was more than 10%, it was recalculated. The average finding of the two observers was the final immunohistological data.

Image analysis

The enhancement patterns of hypo-, iso-, or hyperattenuation were qualitatively defined by comparing each surrounding liver parenchyma in the hepatic arterial phase (HAP). Using the following criteria, each lesion was classified into one of three groups: (1) the hypovascular group, in which nodules demonstrated iso- to hypo-attenuation without hyperattenuation areas in the HAP; (2) the rim-enhancement group, in which nodules demonstrated hyperattenuation areas in the tumor peripheral margin measuring <50% of the lesion volume in the HAP; and (3) the hypervascular group, in which nodules demonstrated hyperattenuation areas measuring >50% of the lesion volume in the HAP [19]. In the case of multiple ICC lesions, the largest was evaluated. The enhancement patterns of the nodules in the HAP were evaluated independently by two observers (KY and SI) who were blinded to the clinical background and pathological results of the patients.

Statistical analysis

Standard statistical analyses were used to evaluate descriptive statistics, including means, medians, frequencies, and percentages. Continuous variables were compared using the Mann–Whitney *U*-test and Kruskal–Wallis test. Categorical variables were compared using the χ^2 test or Fisher's exact test. Univariate and multivariate survival analyses were performed using Cox proportional hazard models. Cumulative overall survival (OS) and recurrence-free survival (RFS) rates were calculated using the Kaplan–Meier method, and differences between curves were evaluated using the log-rank test. OS was calculated as the number of years from the date of surgery to the date of the last follow-up or death. To identify postoperative prognostic factors, several variables found to be independent in univariate analyses were included in the overall multivariate Cox proportional model to analyze both OS and RFS. All statistical tests were two-sided, and a value of $P < 0.05$ was considered to indicate statistical significance. All statistical analyses were performed using JMP14 software (SAS Institute, Cary, NC, USA).

Results

The 100 enrolled patients included 68 men and 32 women, the median age was 66 years (range: 33–87 years), and the median OS and RFS times were 3.2 and 1.3 years, respectively. Regarding the etiology of ICC, ten patients had hepatitis B virus infection, and ten patients had hepatitis C virus infection. Eleven of the 100 patients were diagnosed with liver cirrhosis by pathological features.

Of these 100 patients, 77 were treated with complete resection (R0), whereas 23 patients received a nearly complete resection (R1). In our institution, lymph node dissection was performed according to whether lymph node metastasis was suspected on the preoperative abdominal computed tomography (CT) scan [20]. Pathological examinations revealed that 23 (43.4%) of the 53 patients who underwent lymph node dissection had lymph node metastasis. Regarding radiological analyses, 74 patients whose enhancement CT images remained in the electronic medical records were enrolled to examine the relationship between the MVD and enhancement CT patterns.

The histopathological definition of cholangiocarcinoma (CCA) was based on the classification proposed by the World Health Organization. CCA is classified into intrahepatic, perihilar, and distal types, based on its biliary tree location. Peripheral and perihilar CCA were diagnosed in 72 and 28 cases, respectively. Peripheral CCA cases were classified into the following subtypes: mass-forming (MF), periductal infiltrating (PI), and intraductal growth (IG) types. Sixty-seven (93.1%), four (5.6%), and one (1.3%) tumor were classified as MF, PI, and IG, respectively. Recently, peripheral and perihilar CCAs have been reported to show similar pathologic characteristics and outcomes [21]. In addition, the large-duct type of ICC may share molecular features with perihilar CCA [22]. Moreover, it is difficult to discriminate perihilar type from peripheral type solely by the tumor location. Perihilar type can develop in the hepatic hilar area, which resembles the perihilar type. Therefore, this study included 28 perihilar CCAs in ICC.

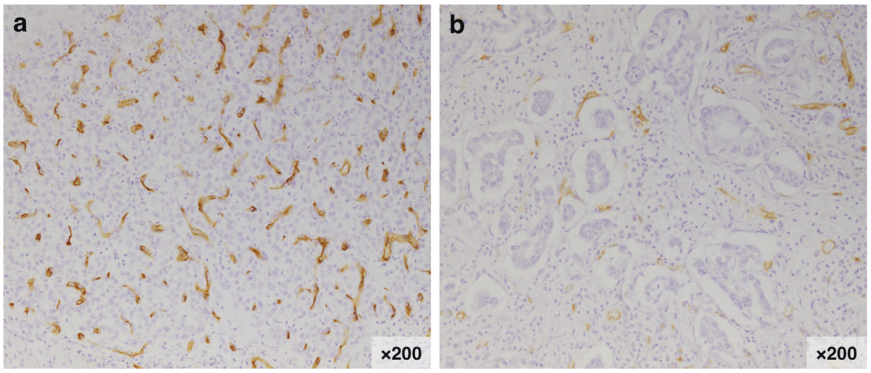

Fig. 1 Representative features of microvessels in intrahepatic cholangiocarcinoma. Cases of intratumoral high ($n = 50$, **a**) and low ($n = 50$, **b**) MVDs (×200 magnification).

Comparison of the clinicopathological characteristics between patients with high and low MVDs

The median MVD in the intratumoral area was 39.5/0.950 mm^2 (range: 7.2–128.6/0.950 mm^2), and a cutoff value of 40.6/0.950 mm^2 was applied using a receiver operating characteristic (ROC) curve (area under the curve, 0.669; sensitivity, 71.1%; specificity, 64.8%, $P = 0.003$). The cutoff value classified 50/100 patients (50.0%) as the high MVD group (≥40.6/0.950 mm^2) and 50/100 patients (50.0%) as the low MVD group (<40.6/0.950 mm^2). Figure 1 shows the representative high and low MVD for the immunohistochemical staining of CD34.

The clinicopathological characteristics of patients in the high and low MVD groups are shown in Table 1. Overall, the serum platelet counts and carbohydrate antigen 19-9 (CA19-9) levels were high in patients with low MVDs compared with those with high MVDs (median 13.3 vs. 21.6×10^4/μL, $P = 0.017$; median 34.9 vs. 90.4 U/mL, $P = 0.008$). The patients with a low MVD had a significantly larger tumor size (median 3.5 vs. 5.0 cm, $P = 0.016$) than those with a high MVD. Moreover, microvascular invasion and intrahepatic and lymph node metastasis were more frequently observed in patients with low MVDs than in those with high MVDs [18/50 (36.0%) vs. 34/50 (68.0%), $P = 0.001$; 13/50 (26.0%) vs. 24/50 (48.0%), $P = 0.023$; 4/50 (8.0%) vs. 19/50 (38.0%), $P < 0.001$, respectively].

Comparison of each attenuation pattern on enhancement CTs between patients with high and low MVDs

In addition, the relationship between the intratumoral MVD and radiological features of attenuation patterns in the HAP on enhancement CTs was confirmed. According to the above criteria [19], the attenuation patterns in ICCs were classified as hypovascular (hypo, $n = 28$), rim-enhancement (rim, $n = 27$), and hypervascular (hyper, $n = 19$) types (Fig. 2a). The attenuation patterns were significantly correlated with the MVD in ICCs ($P < 0.001$; Fig. 2b). ICCs with low MVDs were significantly reflected as hypovascular lesions on enhancement CTs compared with ICCs with high MVDs [ratio of hypovascular lesions: 7/42 (16.7%) vs. 21/32 (65.6%), $P < 0.001$]. Furthermore, as shown in Supplementary Fig. 1, the patients with hypervascular lesions in ICCs on enhancement CTs showed favorable prognoses compared with the hypo- and rim-enhancement groups (OS, $P = 0.059$; RFS, $P = 0.043$).

Relationships between the MVD, CD8+ and Foxp3+ TILs, and PD-L1

Next, the relationships between the MVD, CD8+ and Foxp3+ TILs, and PD-L1 expression in cancer cells in ICC tissues were clarified. According to the consensus evaluation of TILs [18], the proportion of infiltrating intratumoral inflammatory cells was variable in ICC tissues (Fig. 3a). Interestingly, a highly statistically significant relationship was observed between the MVD and intratumoral TIL count ($r = 0.562$, $P < 0.001$; Fig. 3b).

Accordingly, immunohistochemical staining was performed to confirm the detailed distribution of T lymphocytes. The ICC patients with low MVDs had higher CD8+ and lower Foxp3+ TIL counts than those with high MVDs (median CD8+ TIL counts: 19.9 vs. 24.8 cells/0.237 mm^2; median Foxp3+ TIL counts: 7.6 vs. 3.9 cells/0.237 mm^2). More importantly, highly statistically significant relationships were observed between the MVD and CD8+ TIL count ($r = 0.754$, $P < 0.001$; Fig. 3c, d) and Foxp3+ TIL count ($r = -0.302$, $P = 0.003$; Fig. 3d, e). Cutoff values of CD8+ and Foxp3+ TILs were decided based on the respective median values (25.5 cells/0.237 mm^2 for CD8+ and 5.0 cells/0.237 mm^2 for Foxp3+) for further prognostic analysis. The clinicopathological characteristics of patients in the high and low CD8+ TIL and Foxp3+ TIL groups are shown in Supplementary Table 1. Moreover, PD-L1 expression levels in ICC cells were evaluated by IHC. The cutoff point for PD-L1 expression was defined at 1% of

Table 1 Comparison of the clinicopathological factors between patients with high and low microvessel densities (MVDs) following hepatic resection of intrahepatic cholangiocarcinoma.

Factors	High MVD ($n = 50$)	Low MVD ($n = 50$)	P value
Age (years)	65 (33–82)	67 (39–87)	0.424
Sex (male/female)	35/15	33/17	0.668
HBV (+, %)	4 (8.0%)	6 (12.0%)	0.505
HCV (+, %)	5 (10.0%)	5 (10.0%)	1.000
Albumin (g/dL)	4.1 (3.2–5.3)	4.1 (2.9–4.7)	0.729
Total bilirubin (mg/dL)	0.7 (0.2–1.8)	0.7 (0.4–8.7)	0.637
ALP (U/L)	307.0 (127–1344)	351.5 (125–1337)	0.143
γ-GTP (IU/L)	76.5 (24–574)	94.5 (11.7–1071)	0.508
Platelets ($\times 10^4/\mu L$)	13.3 (5.2–44.0)	21.6 (10.4–54.3)	0.017*
Total lymphocytes ($\times 10^3/uL$)	1.5 (0.4–4.0)	1.4 (0.4–2.8)	0.391
ICG15 (%)	11.6 (1.9–31.0)	9.1 (2.3–23.6)	0.179
CEA (ng/mL)	2.8 (0.0–117.5)	2.6 (0.4–30.7)	0.664
CA19-9 (U/mL)	34.9 (0.0–531.9)	90.4 (0.6–98106)	0.008*
Tumor size (cm)	3.5 (0.5–12.0)	5.0 (1.7–9.5)	0.016*
Tumor localization (peripheral type/perihilar type)	40/10	32/18	0.075
ICC subtype ($n = 72$) MF/PI/IG	38/2/0	29/2/1	0.426
Poor differentiation (%)	27 (54.0%)	32 (64.0%)	0.309
Microvascular invasion (%)	18 (36.0%)	34 (68.0%)	0.001*
Bile duct invasion (%)	19 (38.0%)	23 (46.0%)	0.418
Intrahepatic metastasis (%)	13 (26.0%)	24 (48.0%)	0.023*
Lymph node metastasis (%)	4 (8.0%)	19 (38.0%)	<0.001**
Histological liver cirrhosis (%)	7 (14.0%)	4 (8.0%)	0.338

Data are presented as n (%) or the median (range).

ALP alkaline phosphatase, *CA19-9* carbohydrate antigen 19-9, *CEA* carcinoembryonic antigen, *γ-GTP* γ-glutamyl transpeptidase, *HBV* hepatitis B virus, *HCV* hepatitis C virus, *ICG15* indocyanine green retention rate at 15 min, *IG* intraductal growth, *MF* mass-forming, *MVD* microvessel density, *PI* periductal infiltrating.

*$P < 0.05$; **$P < 0.001$.

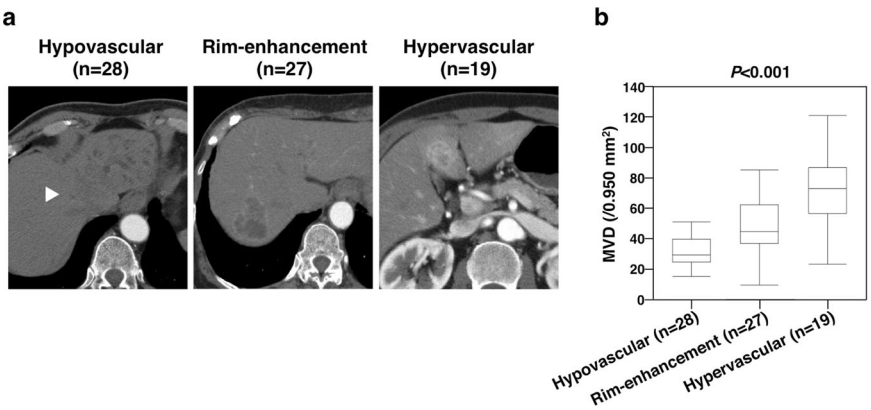

Fig. 2 Representative features and comparison of each attenuation pattern on enhancement CTs ($n = 74$). **a** In the arterial phase, hypovascular lesions ($n = 28$, white arrowhead), rim-enhancement ($n = 27$), and hypervascular lesions ($n = 19$) were observed on enhancement CTs. **b** Correlation between the MVD and each attenuation pattern on enhancement CTs.

total cancer cells as previously described [23], and the patients were divided into PD-L1 negative ($n = 51$) and PD-L1 positive ($n = 49$) groups (Fig. 4a, b). There were no significant differences between PD-L1 expression and MVDs or CD8+ and Foxp3+ TILs (Fig. 4c).

Regarding the degree of fibrosis and necrosis, the proportion of fibrosis was classified as mild ($n = 66$), moderate ($n = 23$), and severe ($n = 11$) in the ICC stroma (Fig. S2a). Fifty-one ICCs showed necrosis, and 49 showed no necrosis (Fig. S2b). No significant difference was found between the

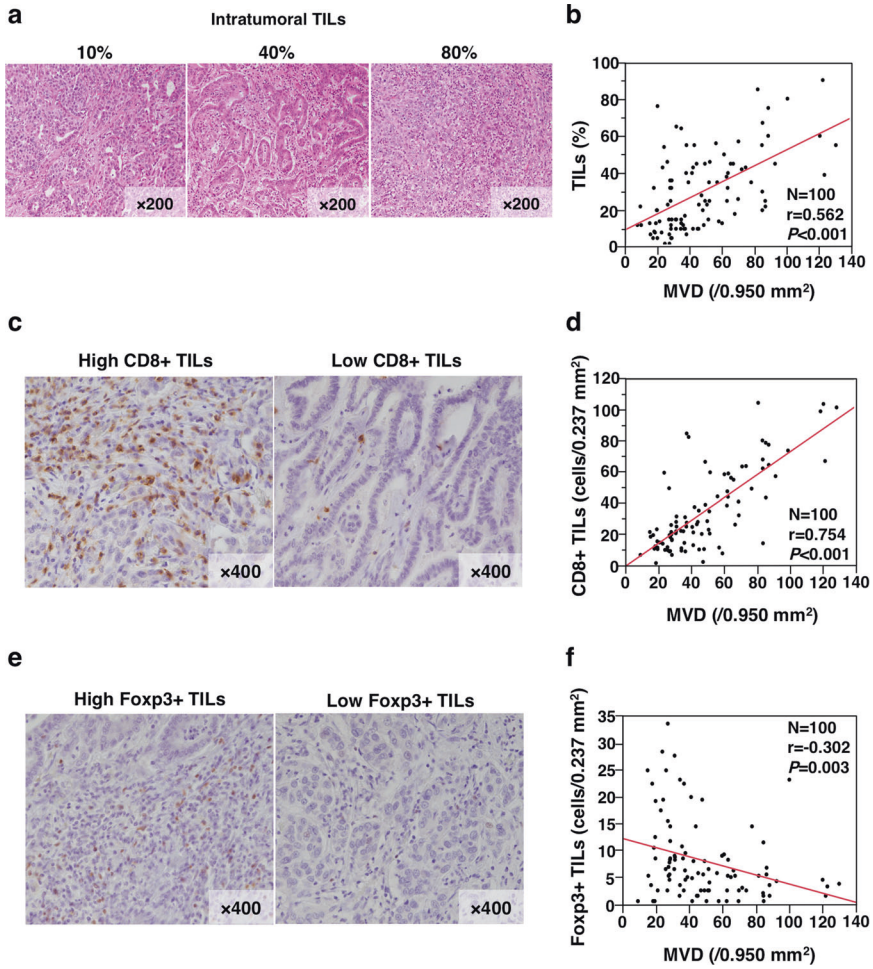

Fig. 3 Representative features of CD8 and Foxp3 immunohistochemically staining and comparisons of the MVD and each immunohistochemical finding. **a** Variable features of intratumoral TILs (×200 magnification). **b** Relationship between the MVD and TILs. **c** Representative features of high and low CD8+ TILs and **d** relationship between the MVD and CD8+ TILs. **e** Representative features of high and low Foxp3+ TILs (×400 magnification). **f** Relationship between the MVD and Foxp3+ TILs.

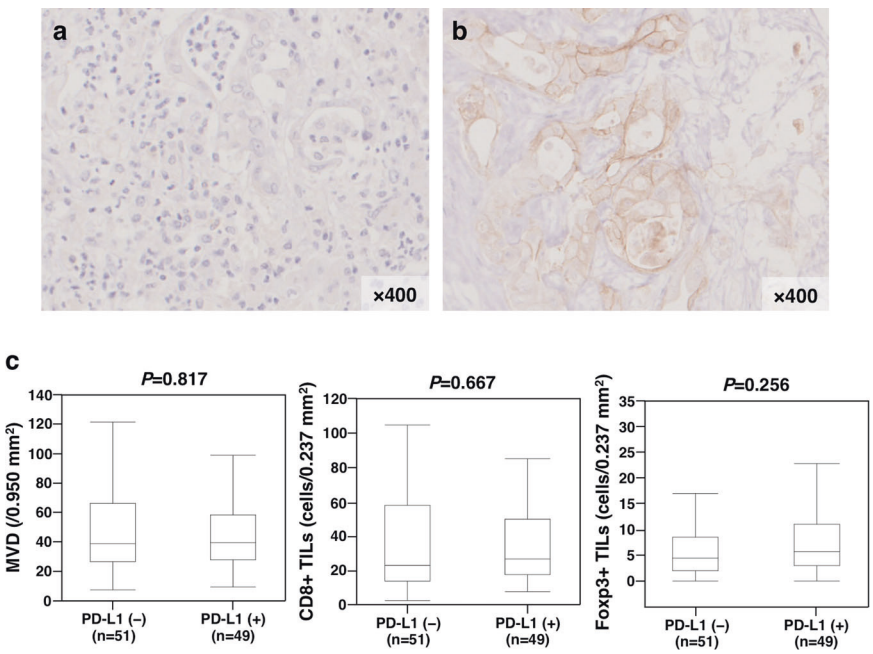

Fig. 4 Representative features of PD-L1 expression in intrahepatic cholangiocarcinoma. PD-L1 negative ($n = 51$, **a**) and positive ($n = 49$, **b**) cases (×200 magnification). **c** Relationships between PD-L1 expression and MVDs and CD8+ and Foxp3+ TILs.

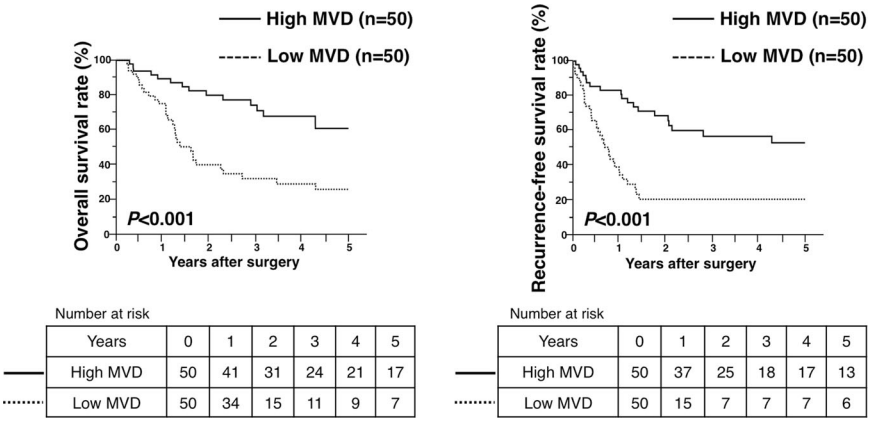

Number at risk

	Years	0	1	2	3	4	5
—	High MVD	50	41	31	24	21	17
·····	Low MVD	50	34	15	11	9	7

Number at risk

	Years	0	1	2	3	4	5
—	High MVD	50	37	25	18	17	13
·····	Low MVD	50	15	7	7	7	6

Fig. 5 Relationship between MVD and overall and recurrence-free survival in ICC patients who underwent hepatic resection. The solid line shows survival in patients with high MVD and the dotted line shows survival in patients with low MVD.

MVD and fibrosis ($P = 0.835$; Fig. S2c). Necrosis was also not significantly related to the MVD ($P = 0.058$; Fig. S2d).

Prognosis analysis of patients with ICC according to the MVD, CD8 + and Foxp3 + TILs, and PD-L1

The OS and RFS curves for patients with high and low MVDs are shown in Fig. 5. Patients with a low MVD had a significantly worse prognosis than those with a high MVD for both OS and RFS (median OS time: 1.6 vs. 7.4 years, $P < 0.001$; median RFS time: 0.7 vs. 8.8 years, $P < 0.001$) (Fig. 5). The OS and RFS curves with respect to CD8+ and Foxp3+ TIL counts and PD-L1 expression are shown in Supplementary Fig. 3. Patients with a low CD8+ TIL count had a significantly worse RFS than those with a high CD8+ TIL count (median RFS time: 1.0 vs. 4.2 years, $P = 0.023$) and tended to show a worse, but not statistically significant, OS (median OS time: 2.7 vs. 6.0 years, $P = 0.090$) (Fig. S3a). Patients with a high Foxp3+ TIL count had a significantly worse prognosis than those with a low Foxp3+ TIL count for OS (median OS time: 2.3 vs. 6.0 years, $P = 0.045$) but not for RFS (median RFS time: 1.0 vs. 2.8 years, $P = 0.051$) (Fig. S3b). Patients with high PD-L1 expression had a significantly worse prognosis than those with low PD-L1 expression for OS (median OS time: 1.9 vs. 7.4 years, $P = 0.048$) but not for RFS (median RFS time: 1.4 vs. 1.1 years, $P = 0.521$) (Fig. S3c).

To evaluate clinical continuous variables, the following cutoff values were decided using ROC curves: 54 years for the patient's age, 4.0 g/dL for the serum albumin level, 2.1 ng/mL for the serum carcinoembryonic antigen (CEA), 84.6 U/mL for the serum CA19-9 level, and 3.2 cm for the tumor size. The 28 cases of perihilar type were excluded from the prognostic analysis. Univariate analyses showed that the significant prognostic factors for OS were low MVD, low CD8+ TIL count, PD-L1 positivity, large tumor size (≥3.2 cm), positivity for microvascular invasion, and intrahepatic and lymph node metastases. Univariate analyses showed that the significant prognostic factors for RFS were low MVD, low CD8+ TIL count, high serum CA19-9 level (≥84.6 U/mL), large tumor size (≥3.2 cm), positivity for microvascular invasion, and intrahepatic and lymph node metastases. Multivariate analysis identified PD-L1 positivity, large tumor size (≥3.2 cm), and positivity for lymph node metastasis as significant prognostic factors that influenced OS and low MVD and positivity for intrahepatic metastasis as significant prognostic factors that influenced RFS (Table 2).

Discussion

In the current study, we first determined that a low intratumoral MVD is a significant predictive factor in patients with ICC. In addition to histological evaluations, a hypovascular lesion on an enhancement CT significantly reflects a low MVD in ICC tissues. Furthermore, a low intratumoral MVD is strongly correlated with low CD8+ and high Foxp3+ TIL counts, whereas no significant correlations were found with fibrosis, necrosis, and PD-L1 expression in cancer cells. Taken together, a decreased intratumoral MVD is significantly associated with ICC progression, possibly by altering the recruitment of intratumoral TILs.

Previous studies have demonstrated that tumor microvessels predict a poor prognosis in ICC patients who have undergone radical resection. However, discrepancies exist among these results. Some reports showed that high MVD was associated with poor prognosis in ICC patients [24–26]. On the other hand, Aishima et al. showed that a decreased intratumoral arterial vessel density significantly reflected aggressive tumor behavior and poor prognoses in ICC patients [27]. Nanashima et al. also showed that a lower microvessel count was correlated with tumor malignancy in 37 ICC patients [28]. Consistent with these results, we confirmed that low MVDs were highly associated with a worse prognosis of ICC patients than those with high MVDs. Tumor angiogenesis has been described as a modulator of tumor malignant activities in several

Table 2 Univariate and multivariate analyses of risk factors for overall and recurrence-free survival following hepatic resection of peripheral cholangiocarcinoma.

Factors	Overall survival				Recurrence-free survival			
	Univariate analysis		Multivariate analysis		Univariate analysis		Multivariate analysis	
	HR (95% CI)	*P* value	HR (95% CI)	*P* value	HR (95% CI)	*P* value	HR (95% CI)	*P* value
Low MVD	2.82 (1.30–6.13)	0.009*	2.21 (0.25–2.25)	0.177	2.97 (1.42–6.21)	0.004*	3.77 (1.38–10.3)	0.010*
Low CD8+ TILs	2.59 (1.20–5.60)	0.015*	0.75 (0.24–2.25)	0.601	2.33 (1.18–4.59)	0.015*	0.47 (0.18–1.23)	0.123
High Foxp3+ TILs	1.30 (0.63–2.70)	0.480			1.11 (0.58–2.14)	0.750		
PD-L1 positive	2.54 (1.15–5.61)	0.021*	2.70 (1.06–6.87)	0.037*	1.35 (0.70–2.61)	0.371		
Age (≥54)	0.68 (0.31–1.51)	0.341			0.60 (0.28–1.27)	0.181		
Male	1.21 (0.54–2.73)	0.647			1.48 (0.70–3.15)	0.307		
Albumin (<4.0 g/dL)	1.86 (0.90–3.86)	0.096			1.39 (0.72–2.71)	0.327		
CA19-9 (≥84.6 U/mL)	2.13 (0.98–4.64)	0.056			2.02 (1.00–4.07)	0.049*	0.85 (0.35–2.08)	0.727
Tumor size (≥3.2 cm)	7.05 (1.67–29.7)	0.008*	5.39 (1.17–24.7)	0.030*	3.78 (1.46–9.77)	0.006*	2.44 (0.82–7.29)	0.109
Poor differentiation	1.14 (0.54–2.42)	0.729			1.31 (0.66–2.60)	0.432		
Microvascular invasion (+)	2.87 (1.26–6.53)	0.012*	1.97 (0.75–5.12)	0.167	2.73 (1.36–5.50)	0.005*	1.61 (0.68–3.83)	0.276
Bile duct invasion (+)	1.51 (0.73–3.15)	0.268			1.05 (0.53–2.08)	0.883		
Intrahepatic metastasis (+)	3.24 (1.54–6.81)	0.002*	1.60 (0.71–3.62)	0.258	3.39 (1.74–6.58)	<0.001**	2.44 (1.05–5.70)	0.039*
Lymph node metastasis (+)	3.76 (1.65–8.58)	0.002*	7.36 (2.19–24.8)	0.001*	2.33 (1.01–5.36)	0.046*	2.31 (0.73–7.26)	0.153
Histological liver cirrhosis (+)	1.75 (0.66–4.63)	0.258			1.39 (0.54–3.61)	0.495		

CA19-9 carbohydrate antigen 19-9, *CD8* cluster of differentiation 8, *CI* confident interval, *Foxp3* forkhead box protein P3, *HR* hazard ratio, *MVD* microvessel density, *PD-L1* programmed death-ligand 1, *TILs* tumor-infiltrating lymphocytes.

*$P < 0.05$; **$P < 0.001$.

cancer types because it provides the route for microvascular invasion and metastasis and maintains tumor conditions such as oxygen and nutrients. Our results demonstrated that a high blood supply is not always associated with ICC progression. In the current population, the tumor size of the low MVD group was significantly larger than that of the high MVD group, which suggests that low vascularity may affect tumor growth. Tumor angiogenesis may be necessary for tumor growth at an early stage, but at the advanced stage, the decreased microvessels may have some effect on tumor progression.

Recent studies found that ICCs showed typical hypovascular lesions, and patients with hypovascular lesions in the HAP had significantly poor prognoses [19, 29]. Consistent with these findings, our results that ICCs with hypovascular lesions on enhancement CTs significantly reflected low MVDs in ICC tissues and poor prognoses are plausible. The enhancement patterns on CT strongly correlated with the intratumoral MVD; therefore, it might be a prognostic predictor in the preoperative assessment. Thus, a histological MVD evaluation combined with radiological enhancement patterns on CTs can be helpful to stratify risk among ICC patients.

As cited above, an increasing number of studies have demonstrated that tumor angiogenesis is associated with poor prognosis in patients with ICC; however, the detailed association between tumor microvessels and ICC progression has not been fully elucidated. In this study, we evaluated the relationship between the MVD and TILs, revealing a high correlation between the MVD and CD8+ and Foxp3+ TIL counts. In ICC, Vigano et al. found that CD3+ and CD8+ TILs were associated with higher survival and lower recurrence rates, whereas Foxp3+ TILs were associated with a worse prognosis [30]. Consistent with this finding, our results provided evidence that low CD8+ and high Foxp3+ TIL counts were associated with a poor prognosis in ICC patients. Importantly, we identified that intratumoral MVDs showed a strong positive correlation with the CD8+ TIL count and a negative correlation with the Foxp3+ TIL count in ICC. These findings suggest that tumor microvessels might regulate antitumor immunity through the attenuation of cytotoxic TILs and activation of regulatory TILs in ICC.

Recently, immune checkpoint inhibitors (ICIs) have been highlighted as an effective treatment strategy for several cancers [31]. In HCC, we and others previously reported that PD-L1 expression in cancer cells was associated with a poor clinical outcome [23, 32, 33]. However, the prognostic impact of PD-L1 expression in ICC patients remains controversial [16, 34, 35]. Our results showed that PD-L1 expression was associated with poor prognoses in ICC patients. Relationships between PD-L1

expression in ICC cells and CD8+ and Foxp3+ TILs and microvessels were not found in this study. These results suggest that PD-L1 expression in cancer cells might be involved in epigenetic mechanisms that are unique to ICC cells, not the effects of the immune status in TMEs. However, the number of TILs and level of PD-L1 expression in ICC suggested that ICIs might provide effective treatment.

This study has some potential limitations. First, this was a single-center and long-term retrospective study designed to examine prognostic factors influencing OS and RFS. This case series included patients treated in postoperative adjuvant chemotherapy, which might influence their long-term outcomes. Second, our findings suggest that cancer-associated ECs can produce some mediators and regulate the antitumor immune response in ICC. However, we did not examine the detailed mechanisms. Finally, all other distributions of tumor-infiltrating immune cells and factors that affect angiogenesis were not clarified, all of which require further work.

Acknowledgements We would like to thank Ms. Saori Tsurumaru, Ms. Asuka Nakamura, Ms. Yuko Kubota, and Ms. Miki Nakashima for their technical support. We thank Melissa Crawford, Ph.D., from Edanz Group (https://en-author-services.edanzgroup.com/) for editing a draft of this paper.

Funding This study was supported by the following three grants: JSPS KAKEN Grant (Number JP-16K10576 and JP-19K09198); and the program for Basic and Clinical Research on Hepatitis from Japan Agency for Medical Research and Development, AMED. The funding sources had no role in the collection, analysis, or interpretation of the data, or in the decision to submit the article for publication.

Compliance with ethical standards

Conflict of interest The authors declare that they have no conflict of interest.

Publisher's note Springer Nature remains neutral with regard to jurisdictional claims in published maps and institutional affiliations.

References

1. Siegel R, Ma J, Zou Z, Jemal A. Cancer statistics, 2014. CA Cancer J Clin. 2014;64:9–29.
2. Patel T. Increasing incidence and mortality of primary intrahepatic cholangiocarcinoma in the United States. Hepatology. 2001;33:1353–7.
3. Sakamoto Y, Kokudo N, Matsuyama Y, Sakamoto M, Izumi N, Kadoya M, et al. Proposal of a new staging system for intrahepatic cholangiocarcinoma: analysis of surgical patients from a nationwide survey of the Liver Cancer Study Group of Japan. Cancer. 2016;122:61–70.
4. Farges O, Fuks D, Le Treut YP, Azoulay D, Laurent A, Bachellier P, et al. AJCC 7th edition of TNM staging accurately discriminates outcomes of patients with resectable intrahepatic cholangiocarcinoma: By the AFC-IHCC-2009 study group. Cancer. 2011;117:2170–7.
5. Job S, Rapoud D, Dos Santos A, Gonzalez P, Desterke C, Pascal G, et al. Identification of four immune subtypes characterized by distinct composition and functions of tumor microenvironment in intrahepatic cholangiocarcinoma. Hepatology. 2019. https://doi.org/10.1002/hep.31092. Online ahead of print.
6. Sirica AE. The role of cancer-associated myofibroblasts in intrahepatic cholangiocarcinoma. Nat Rev Gastroenterol Hepatol. 2011;9:44–54.
7. Zeng J, Liu Z, Sun S, Xie J, Cao L, Lv P, et al. Tumor-associated macrophages recruited by periostin in intrahepatic cholangiocarcinoma stem cells. Oncol Lett. 2018;15:8681–6.
8. Hida K, Maishi N, Annan DA, Hida Y. Contribution of tumor endothelial cells in cancer progression. Int J Mol Sci. 2018;19:1272.
9. Sabbatino F, Villani V, Yearley JH, Deshpande V, Cai L, Konstantinidis IT, et al. PD-L1 and HLA Class I antigen expression and clinical course of the disease in intrahepatic cholangiocarcinoma. Clin Cancer Res. 2016;22:470–8.
10. Barnes TA, Amir E. HYPE or HOPE: the prognostic value of infiltrating immune cells in cancer. Br J Cancer. 2017;117:451–60.
11. Tanaka A, Sakaguchi S. Regulatory T cells in cancer immunotherapy. Cell Res. 2017;27:109–18.
12. Kinoshita F, Takada K, Yamada Y, Oku Y, Kosai K, Ono Y, et al. Combined evaluation of tumor-infiltrating CD8+ and FoxP3+ lymphocytes provides accurate prognosis in stage IA lung adenocarcinoma. Ann Surg Oncol. 2019;27:2102–9.
13. Suzuki H, Chikazawa N, Tasaka T, Wada J, Yamasaki A, Kitaura Y, et al. Intratumoral CD8+ T/FOXP3+ cell ratio is a predictive marker for survival in patients with colorectal cancer. Cancer Immunol Immunother. 2009;59:653–61.
14. Miyashita M, Sasano H, Tamaki K, Hirakawa H, Takahashi Y, Nakagawa S, et al. Prognostic significance of tumor-infiltrating CD8+ and FOXP3+ lymphocytes in residual tumors and alterations in these parameters after neoadjuvant chemotherapy in triple-negative breast cancer: a retrospective multicenter study. Breast Cancer Res. 2015;17:124.
15. Asahi Y, Hatanaka KC, Hatanaka Y, Kamiyama T, Orimo T, Shimada S, et al. Prognostic impact of CD8+ T cell distribution and its association with the HLA class I expression in intrahepatic cholangiocarcinoma. Surg Today. 2020;50:931–40.
16. Jing CY, Fu YP, Yi Y, Zhang MX, Zheng SS, Huang JL, et al. HHLA2 in intrahepatic cholangiocarcinoma: an immune checkpoint with prognostic significance and wider expression compared with PD-L1. J Immunother Cancer. 2019;7:77.
17. Xu G, Sun L, Li Y, Xie F, Zhou X, Yang H, et al. The clinicopathological and prognostic value of PD-L1 expression in cholangiocarcinoma: a meta-analysis. Front Oncol. 2019;9:897.
18. Hendry S, Salgado R, Gevaert T, Russell PA, John T, Thapa B. et al. Assessing tumor-infiltrating lymphocytes in solid tumors: a practical review for pathologists and proposal for a standardized method from the international immunooncology biomarkers working group: part 1: assessing the host immune response, TILs in invasive breast carcinoma and ductal carcinoma in situ, metastatic tumor deposits and areas for further research. Adv Anat Pathol. 2017;24:235–51.
19. Fujita N, Asayama Y, Nishie A, Ishigami K, Ushijima Y, Takayama Y, et al. Mass-forming intrahepatic cholangiocarcinoma: enhancement patterns in the arterial phase of dynamic hepatic CT—correlation with clinicopathological findings. Eur Radiol. 2017;27:498–506.
20. Yugawa K, Itoh S, Kurihara T, Yoshiya S, Mano Y, Takeishi K, et al. Skeletal muscle mass predicts the prognosis of patients with intrahepatic cholangiocarcinoma. Am J Surg. 2019;218:952–8.
21. Ercolani G, Dazzi A, Giovinazzo F, Ruzzenente A, Bassi C, Guglielmi A, et al. Intrahepatic, peri-hilar and distal

cholangiocarcinoma: three different locations of the same tumor or three different tumors? Eur J Surg Oncol. 2015;41:1162–9.
22. Akita M, Sofue K, Fujikura K, Otani K, Itoh T, Ajiki T, et al. Histological and molecular characterization of intrahepatic bile duct cancers suggests an expanded definition of perihilar cholangiocarcinoma. HPB. 2019;21:226–34.
23. Itoh S, Yoshizumi T, Yugawa K, Imai D, Yoshiya S, Takeishi K, et al. Impact of immune response on outcomes in hepatocellular carcinoma: association with vascular formation. Hepatology. 2020. https://doi.org/10.1002/hep.31206. Online ahead of print.
24. Shirabe K, Shimada M, Tsujita E, Aishima S, Maehara S, Tanaka S, et al. Prognostic factors in node-negative intrahepatic cholangiocarcinoma with special reference to angiogenesis. Am J Surg. 2004;187:538–42.
25. Thelen A, Scholz A, Benckert C, Schroder M, Weichert W, Wiedenmann B, et al. Microvessel density correlates with lymph node metastases and prognosis in hilar cholangiocarcinoma. J Gastroenterol. 2008;43:959–66.
26. Thelen A, Scholz A, Weichert W, Wiedenmann B, Neuhaus P, Gessner R, et al. Tumor-associated angiogenesis and lymphangiogenesis correlate with progression of intrahepatic cholangiocarcinoma. Am J Gastroenterol. 2010;105:1123–32.
27. Aishima S, Iguchi T, Nishihara Y, Fujita N, Taguchi K, Taketomi A, et al. Decreased intratumoral arteries reflect portal tract destruction and aggressive characteristics in intrahepatic cholangiocarcinoma. Histopathology. 2009;54:452–61.
28. Nanashima A, Shibata K, Nakayama T, Tobinaga S, Araki M, Kunizaki M, et al. Relationship between microvessel count and postoperative survival in patients with intrahepatic cholangiocarcinoma. Ann Surg Oncol. 2009;16:2123–9.
29. Ariizumi S, Kotera Y, Takahashi Y, Katagiri S, Chen IP, Ota T, et al. Mass-forming intrahepatic cholangiocarcinoma with marked enhancement on arterial-phase computed tomography reflects favorable surgical outcomes. J Surg Oncol. 2011;104:130–9.
30. Vigano L, Soldani C, Franceschini B, Cimino M, Lleo A, Donadon M, et al. Tumor-infiltrating lymphocytes and macrophages in intrahepatic cholangiocellular carcinoma. Impact on prognosis after complete surgery. J Gastrointest Surg. 2019;23:2216–24.
31. Brahmer JR, Tykodi SS, Chow LQ, Hwu WJ, Topalian SL, Hwu P, et al. Safety and activity of anti-PD-L1 antibody in patients with advanced cancer. N Engl J Med. 2012;366:2455–65.
32. Itoh S, Yugawa K, Shimokawa M, Yoshiya S, Mano Y, Takeishi K, et al. Prognostic significance of inflammatory biomarkers in hepatocellular carcinoma following hepatic resection. BJS Open. 2019;3:500–8.
33. Gabrielson A, Wu Y, Wang H, Jiang J, Kallakury B, Gatalica Z, et al. Intratumoral CD3 and CD8 T-cell densities associated with relapse-free survival in HCC. Cancer Immunol Res. 2016;4:419–30.
34. Gani F, Nagarajan N, Kim Y, Zhu Q, Luan L, Bhaijjee F, et al. Program death 1 immune checkpoint and tumor microenvironment: implications for patients with intrahepatic cholangiocarcinoma. Ann Surg Oncol. 2016;23:2610–7.
35. Zhu Y, Wang XY, Zhang Y, Xu D, Dong J, Zhang Z, et al. Programmed death ligand 1 expression in human intrahepatic cholangiocarcinoma and its association with prognosis and CD8(+) T-cell immune responses. Cancer Manag Res. 2018;10:4113–23.